Resonant Intrachannel Pulse Interactions in Dispersion-Managed Transmission Systems

Mark J. Ablowitz and Toshihiko Hirooka, *Member, IEEE*

***Abstract*—Nonlinear intrachannel interactions in a transmission system with strong periodic dispersion management are investigated. An analytical model that describes the fluctuation of the temporal position and amplitude of the main signal and ghost pulse generation at zero bits due to intrachannel crosstalk is developed. Intrachannel nonlinear effects are found to be a resonant process which is induced by periodic forcing due to lumped amplification assisted by temporal phase matching. Explicit formulae to estimate transmission impairments such as timing and amplitude jitter are provided based on the analytical model. The role of distributed amplification to suppress intrachannel nonlinear effects is also discussed. A more fundamental analytical framework which enables one to evaluate intrachannel crosstalk over a wide regime of system configurations is also presented.**

***Index Terms*—Dispersion management, optical fiber communication, optical fiber nonlinearity.**

I. Introduction

TRANSMISSION of return-to-zero (RZ) pulses in strongly dispersion-managed (DM) fibers is a key technology in high bit rate optical communication systems. Strong dispersion management is found to manage fiber nonlinearity and suppress certain nonlinear effects such as self-phase modulation [1], [2] and interchannel crosstalk in wavelength-division-multiplexed (WDM) systems [3]–[5]. Such a system is, hence, commonly referred to as quasi-linear. In quasi-linear transmission, however, residual nonlinearity induces intrachannel crosstalk between adjacent pulses such as their frequency modulation and energy exchange [6], [7]. This is because of their strong overlap due to large pulsewidth breathing, associated with a significant variation of local dispersion within a period of dispersion management. Nonlinear intrachannel interactions lead to serious transmission penalties such as fluctuation of the temporal position and amplitude of the main signals (the "1s") [8]–[11] and ghost pulse generation at 0 bits [12]. Suppression of intrachannel crosstalk is a key issue to overcome in order to increase the channel bit rate to 40 Gb/s or beyond.

In this paper, we present an analytical model that describes intrachannel nonlinear effects in quasi-linear transmission with strong dispersion management where the local dispersion is varying periodically and the average dispersion is close to zero. Analysis for large and constant dispersion fibers without periodic dispersion compensation was discussed in [13], [14]. As we show in Sections III and IV, periodic dispersion management with small average dispersion [and further extended in Section VII to $O(1)$ average dispersion] results in a resonant situation, so that the evolution of timing and amplitude jitter is significantly different from those discussed in [13], [14]. The strong resonance is introduced by the periodic forcing due to lumped amplification whose period is synchronized with that of dispersion management. The resonant condition is determined by the temporal position of the interacting pulses, which corresponds to phase matching in the frequency domain. Indeed, in the absence of amplification, the intrachannel crosstalk is found to be reduced substantially. In [8], [9], a set of ordinary differential equations (ODEs) were obtained for calculating frequency and amplitude change due to intrachannel crosstalk in periodically DM systems, and then numerically integrated to compute the timing shift and energy change for a fixed bit pattern. Here, we show that the change of the mean frequency, temporal position, and energy of the main signal as well as the amplitude of the ghost pulse grows linearly with respect to distance. The growth rate is obtained as an explicit formula, which allows us to estimate timing and amplitude jitter in pseudorandom bit sequences without need to solve large systems of ODEs. The analytical results compare favorably with the results of direct numerical simulation of the full system. Furthermore, we will outline a multiple scale analysis from which the above theory follows. The multiple scale analysis allows one, in principle, to integrate over longer distances. The analytical framework based on multiple scales covers a wide variety of types of dispersion management including highly dispersed systems [13], [14] and such as those in long-haul dense WDM systems with suitable predispersion and/or postdispersion compensation, where the average dispersion is nonzero in general because of dispersion slope [5], [15].

The remainder of this paper is organized as follows. The perturbed nonlinear Schrödinger (NLS) equation in DM systems on which the analysis of intrachannel crosstalk is based is summarized in Section II. We provide an analytical model to describe nonlinear intrachannel interactions and obtain explicit formulae to compute energy transfer of "1s" and ghost pulse growth in "0s" (Section III) and timing shifts (Section IV) in a fixed bit pattern. Analytical expressions to estimate timing and amplitude jitter are derived in Section V based on the results in Sections III and IV. In Section VI, we discuss the suppression of intrachannel interactions by means of distributed amplification. A more general analytical approach is presented in Section VII, based on multiple scale method which allows one to study intrachannel interactions over longer distance even in the presence of nonzero average dispersion and prechirp.

Manuscript received February 8, 2002; revised March 13, 2002. This work was supported in part by the National Science Foundation under Grant ECS-9800152 and Grant DMS-0101340. The work of T. Hirooka was supported by JSPS Research Fellowships for Young Scientists.

The authors are with the Department of Applied Mathematics, University of Colorado, Boulder, CO 80309-0526 USA (e-mail: hirooka@colorado.edu).

Publisher Item Identifier S 1077-260X(02)05471-0.

II. Perturbed Nonlinear Schrödinger Equation

Propagation of optical pulses in DM fibers in the presence of loss and amplification is described by the perturbed NLS equation

$$i\frac{\partial u}{\partial z}+\frac{D(z)}{2}\frac{\partial^2 u}{\partial t^2}+g(z)|u|^2u=0 \tag{2.1}$$

where all the quantities are expressed in dimensionless units: $t=t_{\rm ret}/t_*$, $z=z_{\rm lab}/z_*$, $u=E/\sqrt{gP_*}$, $D=k''/k''_*$ with the characteristic parameters denoted by the subscript $*$, where $t_{\rm ret}$ and $z_{\rm lab}$ are the retarded time and the propagation distance, respectively, and E denotes the slowly varying envelope of the optical field. The normalizing variables are determined so that $z_*=z_{\rm NL}\equiv 1/\nu P_*$ and $k''_*=-t_*^2/z_{\rm NL}$ where ν is the nonlinear coefficient. We write the signal pulse centered at $t=kT$ as u_k, where T is the bit interval and k is the integer representing the location of the bit slot. The functions $D(z)$ and $g(z)$ describe the local group-velocity dispersion (GVD) of the fiber and the variation of power due to loss and amplification, respectively, which are both periodic in z (with period z_d and z_a, respectively; in this paper, we consider the case $z_a=z_d$ unless otherwise mentioned), and $\langle g\rangle=1$ ($\langle\cdot\rangle$ denotes the path-average over z_a) so that the path-average peak power of pulses is fixed. The nonlinear coefficient $g(z)$ for lumped amplification based on erbium-doped fiber amplifier (EDFA) is given by

$$g(z)=g_e\exp[-2\Gamma(z-nz_a)],\quad nz_a\le z<(n+1)z_a \tag{2.2}$$

where $g_e=4G/[1-\exp(-4G)]$ so that $\langle g\rangle=1$, Γ is the dimensionless loss coefficient, and $G=\Gamma z_a/2$. We write the accumulated dispersion in the form

$$\overline{D}(z)=\int_0^z D(z')\,dz'=C(z)+\langle D\rangle z \tag{2.3}$$

where $\langle D\rangle$ is the average dispersion over a period and $C(z)$ is a periodic function with period z_a having zero average $\langle C(z)\rangle=0$, which also represents the chirp. When $\langle D\rangle$ is not negligible but small, the accumulated dispersion can still be approximated by $\overline{D}\sim C(z)$. In what follows, we consider the case of $\langle D\rangle=0$ unless otherwise mentioned. An analytical model for $\langle D\rangle\neq 0$ is introduced in Section VII.

In order to study nonlinear intrachannel interactions between the main signal u_0 and the adjacent pulses u_l, u_m, u_n, we write $u=u_0+u_l+u_m+u_n$ and substitute this into (2.1) to find the evolution of u_0 perturbed by one of the nonlinear terms $u_l^*u_mu_n$:

$$i\frac{\partial u_0}{\partial z}+\frac{D(z)}{2}\frac{\partial^2 u_0}{\partial t^2}+g(z)|u_0|^2u_0=-g(z)u_l^*u_mu_n. \tag{2.4}$$

The perturbation terms on the right-hand side (RHS) of (2.4) takes two forms, which are either phase-dependent $u_l^*u_mu_n$ ($l\neq m,\,n;\,m,\,n\neq 0$) or phase-independent $|u_n|^2u_0$ ($n\neq 0$). As we discuss in Sections III and IV, phase-dependent terms are responsible for the energy change of u_0 as a result of nonlinear interactions with nonzero bits u_l, u_m, and u_n, whereas phase-independent terms bring about a timing shift of u_0 due to interaction with other nonzero bit u_n.

When $u_0=0$ at $z=0$, nonlinear mixing among u_l, u_m, and u_n can induce the ghost pulse generation at $t=0$. Assuming $u=q+u_l+u_m+u_n$ where q is the ghost pulse at $t=0$ and $|q|\ll 1$, we find a similar equation as (2.4), but linearized in q, which describes the evolution of the ghost pulse

$$i\frac{\partial q}{\partial z}+\frac{D(z)}{2}\frac{\partial^2 q}{\partial t^2}=-g(z)u_l^*u_mu_n. \tag{2.5}$$

The integers l, m and n must satisfy a certain condition to support ghost pulse generation, as we show below.

III. Energy Transfer and Ghost Pulse Generation

In this section, we study the nonlinear interactions due to a phase-dependent forcing term $u_l^*u_mu_n$ ($l\neq m,\,n;\,m,\,n\neq 0$), which yields ghost pulse generation q when the bit is zero and amplitude fluctuation of u_0 when the bit slot is occupied by a signal. They are commonly referred to as intrachannel four-wave mixing (FWM). It should be noted that the phase-independent terms such as $|u_n|^2u_0$ ($n\neq 0$) do not contribute to the ghost pulse growth or energy exchange, since they maintain energy. They are instead responsible for frequency and timing shifts, which will be discussed in Section IV.

A. Phase-Matching Condition

The integers l,m,n representing the bit location of the signals participating in the intrachannel FWM must satisfy a condition in order to induce nonlinear mixing with q or u_0. This is similar to the phase-matching condition in WDM systems [16], but now the frequency matching is replaced by temporal matching.

To obtain the condition in the time domain, let us first consider the simplest case, where the signal pulses are approximated by delta functions $u_k(0,t)=\delta(t-kT)$, corresponding to continuous waves in the frequency domain. Then at a distance z, we have

$$\begin{aligned}u_k(z,t)&=\frac{1}{2\pi}\int_{-\infty}^{\infty}\exp\left[-ikT\omega-iC(z)\omega^2/2+i\omega t\right]d\omega\\&=\sqrt{\frac{1}{2\pi C(z)}}\exp\left[i(t-kT)^2/2C(z)\right].\end{aligned} \tag{3.1}$$

Employing the Fourier transform $\mathcal{F}[u]=\hat{u}(\omega)=\int_{-\infty}^{\infty}u(t)\exp(-i\omega t)\,dt$ of the nonlinear forcing term $F_0(z,t)=-g(z)u_l^*u_mu_n$ in (2.4) or (2.5) implies that

$$\begin{aligned}\hat{F}_0(z,\omega)&=-G(z)\exp\left[-i(m+n-l)\omega T-iC(z)\omega^2/2\right]\\G(z)&=\frac{g(z)}{2\pi C(z)}\exp\left\{i\left[\left(m^2+n^2-l^2\right)-(m+n+l)^2\right]\right.\\&\qquad\left.\times\,T^2/2C(z)\right\}.\end{aligned} \tag{3.2}$$

This indicates that the forcing term $F_0(z,t)$ has a temporal shift of $(m+n-l)T$. When this coincides with $t=0$, namely if

$$l=m+n \tag{3.3}$$

then F_0 induces the ghost pulse growth or the energy change of the signal at $t=0$. When the information bit at $t=0$ is zero,

the ghost pulse q is generated at this location; when the bit is one, u_0 exchanges the energy with u_l, u_m, and u_n.

The extension to more general signal shapes such as Gaussians follows similar lines. If we assume that a signal is given by a Gaussian pulse of the form

$$u_k(z,t)=\frac{\alpha}{\sqrt{2\pi\xi(z)}}\exp\left[-\frac{(t-kT)^2}{2\xi(z)}\right]$$
$$\xi(z)=\beta+iC(z) \tag{3.4}$$

where β is constant, we have

$$\hat{F}_0(z,\omega)=-A(z)\sqrt{\frac{\pi}{a(z)}}\exp\left[-c(z)T^2-\frac{(\omega+ib(z)T)^2}{4a(z)}\right]$$
$$A(z)=\frac{g\alpha^3}{(2\pi)^{3/2}\sqrt{|\xi|^2\xi}},\quad a(z)=\frac{1}{2}\left(\frac{1}{\xi^*}+\frac{2}{\xi}\right)$$
$$b(z)=\frac{l}{\xi^*}+\frac{m+n}{\xi},\quad c(z)=\frac{1}{2}\left(\frac{l^2}{\xi^*}+\frac{m^2+n^2}{\xi}\right). \tag{3.5}$$

$A(z)$, $a(z)$, $b(z)$, and $c(z)$ are periodic complex functions with period z_a. For strong dispersion management, $C\gg 1$ and hence, the forcing term has the temporal shift $bT/2a\sim(m+n-l)T$. This is the same phase-matching condition as for the delta functions.

This phase-matching condition (3.3) is the same as the one found in [13], [14] for large and constant dispersion fibers. However, the periodic nature of dispersion management introduces a further resonance condition, as will be seen in the next subsection.

B. Energy Transfer

Here, we analyze the energy change of the signal u_0 due to nonlinear mixing with u_l, u_m, u_n ($l=m+n$). Differentiating the energy $W_0=\int_{-\infty}^{\infty}|u_0|^2\,dt$ with respect to z, from (2.4) we have an equation for W_0 due to the perturbation $F_0(z,t)$

$$\frac{dW_0}{dz}=-i\int_{-\infty}^{\infty}(F_0u_0^*-F_0^*u_0)\,dt$$
$$=ig(z)\int_{-\infty}^{\infty}(u_0^*u_l^*u_mu_n-\text{c.c.})\,dt. \tag{3.6}$$

Energy change $\Delta W_0(z)=W_0(z)-W_0(0)$ is computed by integration of (3.6). Note that we compute ΔW_0 for all the possible integers $l(=m+n)$, m, n in a given bit pattern and sum them in order to take into account the energy exchange between u_0 and all the other nonzero bits. The formulae to estimate amplitude jitter in a random data sequence will be presented in Section V.

Since the average dispersion $\langle D\rangle$ is small and the pulses u_k are periodic in z because of the periodicity of $D(z)$, and $g(z)$ is varying periodically with the same period, the function dW_0/dz is also periodic in z and thus it can be expanded in a Fourier series of the form $dW_0/dz=\overline{Q}_{m,n}+\sum_{j\neq 0}Q_j\exp(2\pi ijz/z_a)$. Integrating this with respect to z, we note that the mean term $\overline{Q}_{m,n}=(1/z_a)\int_0^{z_a}(dW_0/dz)\,dz$ yields linear growth of the energy change and the other terms in the Fourier series are responsible only for residual oscillations and do not amount to major contributions. As a result, $\overline{Q}_{m,n}z$ is the dominant cause for the growth of the energy change; namely ΔW_0 grows linearly with respect to distance and $\overline{Q}_{m,n}$ represents the growth rate

$$\Delta W_0(z)=\overline{Q}_{m,n}z. \tag{3.7}$$

Thus, we have a resonant growth situation. This does not occur in the large and constant dispersion fiber configuration [13], [14].

In general, when the period of $D(z)$ and $g(z)$ is different, $g(z)$ and $h(z)=\int_{-\infty}^{\infty}(u_0^*u_l^*u_mu_n-\text{c.c.})\,dt$ on the RHS of (3.6) are individually represented as a Fourier series with period z_a and z_d ($\neq z_a$), respectively

$$\frac{dW_0}{dz}=i\left(\sum_{j=-\infty}^{\infty}g_j\exp(2\pi ijz/z_a)\right)$$
$$\times\left(\sum_{k=-\infty}^{\infty}h_k\exp(2\pi ikz/z_d)\right)$$
$$=i\sum_{j,k=-\infty}^{\infty}g_jh_k\exp[2\pi i(j/z_a+k/z_d)z]. \tag{3.8}$$

Among the products on the RHS of (3.8), a resonance is produced from the terms where the phase $\exp[2\pi i(j/z_a+k/z_d)z]$ is canceled, namely

$$jz_d+kz_a=0. \tag{3.9}$$

This is the general condition which yields the resonant growth of energy change ΔW_0. Hereafter in this paper, we consider only the case $z_d=z_a$ (namely $j+k=0$).

So far, no particular restrictions on the form of the pulse shape have been imposed in the analysis. In order to obtain explicit formulae to compute the energy exchange, in the following we assume that a signal is given by a Gaussian pulse (3.4). After substituting (3.4)to (3.6), the mean term $\overline{Q}_{m,n}$ is found to be

$$\overline{Q}_{m,n}=\frac{i\alpha^4}{4\pi^2z_a}\sqrt{\frac{\pi}{2\beta}}\int_0^{z_a}$$
$$\times\left[\frac{g(z)}{|\xi(z)|}\exp\left(-\frac{(m^2+n^2)\beta+2imnC(z)}{2|\xi(z)|^2}T^2\right)\right.$$
$$\left.-\text{c.c.}\right]dz. \tag{3.10}$$

For strong dispersion management, since $C\gg 1$ and hence, $\xi(z)\sim iC(z)$ in (3.10), $\overline{Q}_{m,n}$ can be approximated by

$$\overline{Q}_{m,n}\sim\frac{i\alpha^4}{4\pi^2z_a}\sqrt{\frac{\pi}{2\beta}}\int_0^{z_a}$$
$$\times\left[\frac{g(z)}{|C(z)|}\exp\left(-\frac{imnT^2}{C(z)}\right)-\text{c.c.}\right]dz. \tag{3.11}$$

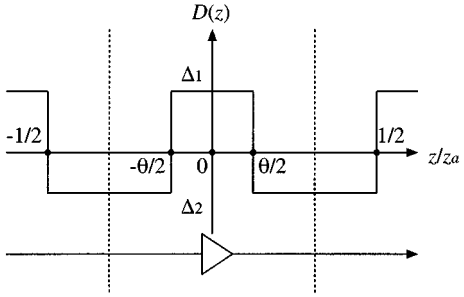

Fig. 1. Schematic diagram of a two-step dispersion map.

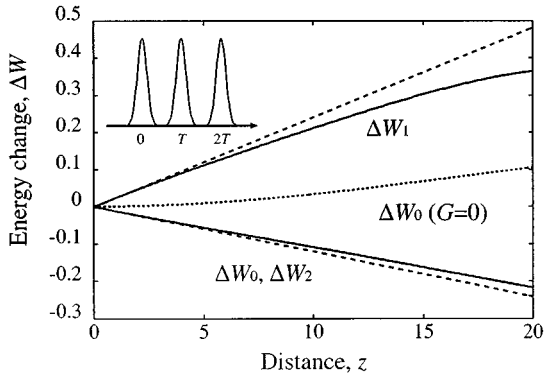

Fig. 2. Growth of energy change of the signals in a 111 bit pattern in a lossy case ($\Gamma = 10$). The solid curves are results of direct numerical simulation of (2.1) and the dashed curves are the results obtained from (3.7) with (3.10). The dotted curve shows the energy change ΔW_0 when $G = 0$ obtained from direct numerical simulation.

To model a dispersion map, we consider a symmetric two-step profile composed of fibers with positive and negative dispersion written as the periodic extension of

$$D(z) = \begin{cases} \Delta, & 0 \le |z| < (\theta/2)z_a \\ -[\theta/(1-\theta)]\Delta, & (\theta/2)z_a \le |z| < (1/2)z_a \end{cases} \tag{3.12}$$

with period z_a (see Fig. 1). In this profile, the dimensionless map strength [1] is defined as $s = \Delta z_a \theta/2$. When $\theta = 1/2$, (3.11) can be simplified to the following:

$$\overline{Q}_{m,n} = \frac{\alpha^4 g_e}{8\pi^2}\sqrt{\frac{\pi}{2\beta}}\,[1-\exp(-2G)]I_{m,n} \tag{3.13a}$$

$$I_{m,n} = \frac{1}{s}\int_{1/s}^{\infty}\left[\exp\left(-\frac{G}{sx}\right)+\exp(-2G)\exp\left(\frac{G}{sx}\right)\right] \times \frac{\sin(mnT^2x)}{x}\,dx. \tag{3.13b}$$

In the limit of $G \to 0$ [i.e., $g(z) = 1$], we note that $\overline{Q}_{m,n} \to 0$. This implies that in a lossless system the energy change is reduced substantially. This observation also holds true for general θ (where the formulae are more complex). This result suggests the possibility of improving transmission performance by employing distributed amplification to suppress intrachannel pulse interactions, which will be demonstrated in Section VI. (See also [17], where the amplitude jitter is found to be suppressed by introducing symmetry in power profile when $\theta = 1/2$.)

Finally, the integral (3.13b) can be asymptotically approximated by the following formula:

$$I_{m,n} \sim \frac{1}{s}\left[(1+\exp(-2G))\left(\frac{\pi}{2}-\frac{1}{\lambda G}\right) - \frac{\log \lambda G}{\lambda}(1-\exp(-2G)) + \frac{1}{\lambda}\left(J_+ + J_-\exp(-2G) - K(1-\exp(-2G))\right)\right], \quad \lambda \gg 1 \tag{3.14}$$

where $\lambda = s/mnT^2G$ (i.e., we allow large s and moderate values of mnT^2), and $J_+ = \int_0^G [\exp(-x) - 1 + x]/x^2\,dx$, $J_- = \int_0^G [\exp(x) - 1 - x]/x^2\,dx$ and $K = \int_0^1 (\sin x - x + x^3/6)/x^2\,dx + \int_1^\infty \sin x/x^2\,dx - 1/12$ are constants.

When $\langle D\rangle \neq 0$, (3.7) must be modified accordingly. Nevertheless, $\Delta W_0(z)$ is found to grow with distance when $\langle D\rangle$ is not negligible but $O(1)$. In fact, the analysis of Section VII shows that the above result is easily modified by replacing $C(z)$ in (3.4) by $C(z) + \langle D\rangle z + C_0$ where we assume $|C| \gg 1$, $\langle D\rangle = O(1)$, where C_0 is the initial chirp. Furthermore, we note that if $\langle D\rangle \gg 1$ (cf. [13], [14]), then the resonant condition (3.9) is violated.

Fig. 2 shows plots of the energy change of the bits u_0, u_1, and u_2 for the bit pattern "111" ($k = 0, 1, 2$; see the inset) and 0 elsewhere, obtained from (3.7) with (3.10) calculated numerically and from direct simulation of (2.1). The parameters that are used in the calculation are $\alpha = \sqrt{2\pi}$, $\beta = 1.0$, $T = 8.3$, $\Gamma = 10$, $z_a = 0.1$, and $s = 22$ in dimensionless units. With the choice of $t_* = 3$ ps, $\nu = 2.5$ W^{-1}·km^{-1}, $P_* = 1$ mW, i.e., $z_{\rm NL} = 400$ km and $k_*''(=-t_*^2/z_{\rm NL}) = -2.25 \times 10^{-2}$ ps^2/km, they correspond to the transmission of the pulses with the path-average peak power 1 mW, the full-width at half-maximum (FWHM) $\tau_{\rm FWHM} = 5$ ps (minimum), and the bit interval $t_{\rm bit} = 25$ ps (corresponding to the bit rate $B = 40$ Gb/s), in a DM fiber with the period 40 km, $k'' = \pm 20$ ps^2/km, and the loss 0.22 dB/km. We note that $\Delta W_2 = \Delta W_0$ and $\Delta W_1 = -2\Delta W_0$ from symmetry and the conservation of total energy. In this case, the only combination of integers satisfying the phase-matching condition is $(l, m, n) = (2, 1, 1)$. Good agreement between the analytical and the numerical results can be seen. It should be noted that over longer distance, as the energy transfer increases, other effects become important and the assumptions in the model must be modified. We also show the energy change of u_0 in a lossless case obtained from direct simulation. As predicted from (3.13), when $G \to 0$ suppression of the energy change is observed even with the same value of path-average signal power as in the lossy case, which further confirms the analysis.

C. Ghost Pulse Growth

We now solve (2.5) to compute the growth of ghost pulse q due to nonlinear mixing among u_l, u_m, u_n ($l = m + n$). The Fourier transform of (2.5) yields

$$i\,\frac{\partial \hat{q}}{\partial z} - \frac{D(z)}{2}\,\omega^2 \hat{q} = \hat{F}_0(z, \omega) \tag{3.15}$$

which is solved as

$$\hat{q}(z,\omega) = i\exp\left[-iC(z)\omega^2/2\right]\int_0^z R(z',\omega)\,dz' \tag{3.16}$$

where $R(z,\omega) = -\hat{F}_0(z,\omega)\exp[iC(z)\omega^2/2]$. Because of the periodicity of each function in $R(z,\omega)$, this can be expanded in the Fourier series of the form $R(z,\omega) = \overline{R}_{m,n}(\omega) + \sum_{j\neq 0} R_j(\omega)\exp(2\pi ijz/z_a)$. We note that the mean term $\overline{R}_{m,n}(\omega) = \langle R(z,\omega)\rangle \equiv (1/z_a)\int_0^{z_a} R(z,\omega)\,dz$ is responsible for the resonant growth of the ghost pulse. The energy of the ghost pulse increases in proportion to z^2

$$W_q(z) = \frac{1}{2\pi}\int_{-\infty}^{\infty}|\hat{q}(z,\omega)|^2\,d\omega = \frac{z^2}{2\pi}\int_{-\infty}^{\infty}\left|\overline{R}_{m,n}(\omega)\right|^2\,d\omega. \tag{3.17}$$

We note that even if the dispersion $D(z)$ contains an average term $\langle D\rangle \neq 0$, we still find resonant-like growth when $\langle D\rangle z \ll C(z)$ in the map. However, the ghost pulse growth is expected to be suppressed with sufficiently large $\langle D\rangle$ such that $\langle D\rangle z \gtrsim C(z)$.

In the following, we assume a signal given by a Gaussian pulse (3.4). For strong dispersion management, since $C(z) \gg 1$ and hence, $\xi(z) \sim iC(z)$, $R(z,\omega)$ can be approximated by

$$\begin{aligned} R(z,\omega) &= A\sqrt{\frac{\pi}{a}}\exp\left[\left(iC-\frac{1}{2a}\right)\frac{\omega^2}{2} - i\frac{bT}{2a}\omega - cT^2 + \frac{b^2T^2}{4a}\right] \\ &\sim \frac{g(z)\alpha^3}{2\pi|C(z)|}\exp\left(-3\beta\omega^2/2 - imnT^2/C\right). \end{aligned} \tag{3.18}$$

The path average $\overline{R}_{m,n}$ of (3.18) in a dispersion map given by (3.12) is

$$\overline{R}_{m,n}(\omega) = \frac{\alpha^3}{2\pi}\exp\left(-3\beta\omega^2/2\right)J_{m,n} \tag{3.19a}$$

$$J_{m,n} = \frac{1}{z_a}\int_0^{z_a}\frac{g(z)}{|C(z)|}\exp\left(-imnT^2/C\right)dz. \tag{3.19b}$$

From (3.16) and (3.19), the ghost pulse for large s is, therefore, approximated by a Gaussian of the form

$$\hat{q}(z,\omega) \sim i\frac{\alpha^3 z}{2\pi}J_{m,n}\exp\left[-(3\beta+iC)\omega^2/2\right] \tag{3.20a}$$

$$q(z,t) \sim i\frac{\alpha^3 z}{2\pi}J_{m,n}\frac{\exp(-t^2/2\xi')}{\sqrt{2\pi\xi'}}, \qquad \xi' \equiv 3\beta + iC(z). \tag{3.20b}$$

When $\theta = 1/2$ in (3.12), $J_{m,n}$ is simplified to the following:

$$\begin{aligned} J_{m,n} = \frac{g_e}{4s}\int_{1/s}^{\infty}&[\exp(-imnT^2x)+\exp(-2G)\exp(imnT^2x)] \\ &\times\left[\exp\left(-\frac{G}{sx}\right)+\exp(-2G)\exp\left(\frac{G}{sx}\right)\right]\frac{dx}{x}. \end{aligned} \tag{3.21}$$

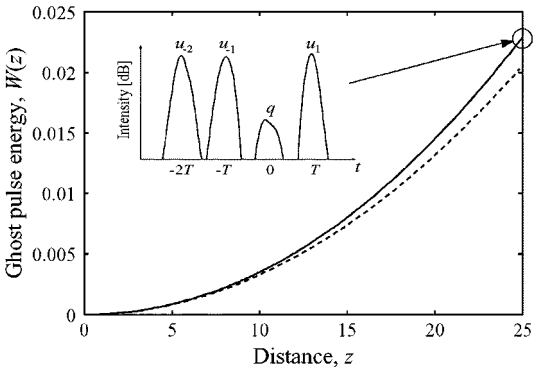

Fig. 3. Growth of ghost pulse energy at the zero bit in a 1101 bit pattern; schematically shown in the inset. The solid curve is a result of direct numerical simulation of (2.1); the dashed curve is the result obtained from (3.17).

Note that, unlike the growth rate of energy change $\overline{Q}_{m,n}$, $\overline{R}_{m,n}$ does not vanish in the limit $G \to 0$. When $G = 0$, we find

$$J_{m,n} = \frac{g_e}{s}\int_{1/s}^{\infty}\frac{\cos\left(mnT^2x\right)}{x}\,dx \tag{3.22}$$

independently of θ. Thus, there still remains ghost pulse generation in a lossless system. However, since (3.22) is asymptotically approximated for large s and moderate values of mnT^2 by

$$J_{m,n} \sim \frac{g_e}{s}\left[\log s - \left(\gamma + \log\left(mnT^2\right)\right) + \cdots\right], \qquad s \gg 1 \tag{3.23}$$

($\gamma = 0.5772$ is the Euler's constant), and for large mnT^2 and small or moderate values of s, by

$$J_{m,n} \sim \frac{g_e}{s}\left[-\frac{\sin\lambda}{\lambda} + \frac{\cos\lambda}{\lambda^2} + \cdots\right], \qquad \lambda \equiv \frac{mnT^2}{s} \gg 1 \tag{3.24}$$

the ghost pulse growth is decreasing for large s or λ.

Fig. 3 shows the ghost pulse growth of the 0 slot in a "1101" bit pattern ($k = -2, -1, 0, 1$; see the inset) due to interaction among u_{-2}, u_{-1}, and u_1. The energy of the ghost pulse is calculated from (3.17) and direct simulation of (2.1). The parameters are the same as in Fig. 2. The combinations of the integers responsible for the ghost pulse standing at $t = 0$ are $(l, m, n) = (-2, -1, -1)$, $(-1, 1, -2)$, and $(-1, -2, 1)$.

IV. Frequency and Timing Shifts

In this section, we study the nonlinear interactions due to a phase-independent forcing term $|u_n|^2u_0$ ($n \neq 0$), which yields the mean frequency shift of a signal, resulting in a shift in its temporal position through fiber dispersion. This is commonly referred to as intrachannel cross-phase modulation (XPM). (See Appendix A for the frequency shift due to intrachannel FWM, which turns out to be negligible.)

The frequency and timing shift of u_0 due to intrachannel XPM with u_n is calculated from the equation

$$i\frac{\partial u_0}{\partial z} + \frac{D(z)}{2}\frac{\partial^2 u_0}{\partial t^2} + g(z)|u_0|^2u_0 = -2g(z)|u_n|^2u_0. \tag{4.1}$$

It is convenient to introduce the following integrals: the mean frequency $\Omega_0 = \mathrm{Im}[\int_{-\infty}^{\infty}(\partial u_0/\partial t)u_0^*\,dt]/W_0$, and the central temporal position $t_0 = \int_{-\infty}^{\infty} t|u_0|^2\,dt/W_0$, where W_0 is the energy of u_0 defined in the previous section. Differentiating Ω_0 and t_0 with respect to z, from (4.1) we find

$$\frac{d\Omega_0}{dz} = \frac{2g(z)\int_{-\infty}^{\infty}|u_0|^2\,\frac{\partial|u_n|^2}{\partial t}\,dt}{\int_{-\infty}^{\infty}|u_0|^2\,dt} \tag{4.2}$$

$$\frac{dt_0}{dz} = D(z)\Omega_0(z). \tag{4.3}$$

The timing shift $\Delta t_0(z) = t_0(z) - t_0(0)$ is obtained by integration of (4.2) with $\Omega_0(0) = 0$ and using (4.3). Note that, in general, we compute Δt_0 corresponding to all the possible integers n in a given bit pattern and sum them in order to evaluate the total amount of timing shift of u_n due to interaction with all the other "1s." The analytical expressions to estimate timing jitter in a random data sequence will be presented in Section IV.

Interchanging the order of integration yields

$$\begin{aligned}\Delta t_0(z) &= \int_0^z D(z')\left[\int_0^{z'}\frac{d\Omega_0}{dz''}\,dz''\right]dz' \\ &= \int_0^z \frac{d\Omega_0}{dz''}\left[\int_{z''}^z D(z')\,dz'\right]dz'' \\ &= \int_0^z \frac{d\Omega_0}{dz''}\left(\overline{D}(z) - \overline{D}(z'')\right)dz'' \\ &= \delta t_0^{(1)}(z) + \delta t_0^{(2)}(z)\end{aligned} \tag{4.4}$$

where

$$\delta t_0^{(1)}(z) = \overline{D}(z)\Omega_0(z) \tag{4.5}$$

$$\delta t_0^{(2)}(z) = \int_0^z\left(-\frac{d\Omega_0}{dz''}\right)\overline{D}(z'')\,dz''. \tag{4.6}$$

Thus the intrachannel timing shift is composed of two terms: $\delta t_0^{(1)}$ and $\delta t_0^{(2)}$. We note that when $\overline{D}(z) = 0$, the timing shift is given by $\delta t_0^{(2)}(z)$ alone in (4.4). In the case of zero average dispersion, this condition corresponds to $C(z) = 0$, namely at chirp-free points. Furthermore when $\langle D\rangle = 0$, $\overline{D}(z) = C(z)$. When the pulse is also periodic in z, the function $(-d\Omega_0/dz)C(z)$ can be expanded in the Fourier series of the form $(-d\Omega_0/dz)C(z) = \overline{P}_n + \sum_{j\neq 0} P_j \exp(2\pi ijz/z_a)$. It follows that the mean term $\overline{P}_n = (1/z_a)\int_0^{z_a}(-d\Omega_0/dz)C(z)\,dz$ is the dominant cause for the growth of the timing shift; from (4.4) and (4.6), the timing shift grows linearly:

$$\delta t_0^{(2)}(z) = \overline{P}_n z. \tag{4.7}$$

In the following, we assume a signal given by a Gaussian pulse (3.4). Substituting (3.4) to (4.2), we have

$$\frac{d\Omega_0}{dz} = \frac{g(z)\alpha^2\beta nT}{\sqrt{2}\pi|\xi(z)|^3}\exp\left(-\frac{\beta n^2T^2}{2|\xi(z)|^2}\right). \tag{4.8}$$

Note that, for strong dispersion management, $C \gg 1$ and hence $\xi(z) \sim iC(z)$. Thus the linear growth rate of $\delta t_0^{(2)}(z)$ is written as

$$\begin{aligned}\overline{P}_n &= -\frac{\alpha^2\beta nT}{\sqrt{2}\pi z_a}\int_0^{z_a}\frac{C(z)g(z)}{|\xi(z)|^3}\exp\left(-\frac{\beta n^2T^2}{2|\xi(z)|^2}\right)dz \\ &\sim -\mathrm{sgn}(C)\,\frac{\alpha^2\beta nT}{\sqrt{2}\pi z_a}\int_0^{z_a}\frac{g(z)}{C^2(z)}\exp\left(-\frac{\beta n^2T^2}{2C^2(z)}\right)dz.\end{aligned} \tag{4.9}$$

In a dispersion map given by a symmetric two-step profile as shown in Fig. 1, when $\theta = 1/2$, (4.9) can be simplified to the following:

$$\overline{P}_n = \frac{g_e}{4}\left[1 - \exp(-2G)\right]A_nI_n \tag{4.10a}$$

$$\begin{aligned}I_n = \frac{1}{s}\int_{1/s}^{\infty}&\left[\exp\left(-\frac{G}{sx}\right) + \exp(-2G)\exp\left(\frac{G}{sx}\right)\right] \\ &\times\exp\left(-\frac{\beta n^2T^2}{2}\,x^2\right)dx\end{aligned} \tag{4.10b}$$

where $A_n = -\alpha^2\beta nT/\sqrt{2}\pi$. In the limit of $G \to 0$ [i.e., $g(z) = 1$], we note that $\overline{P}_n \to 0$, which implies a significant reduction of the timing shift in the lossless case. This also holds true for general θ.

Finally, the integral (4.10b) can be asymptotically approximated by the following formula:

$$\begin{aligned}I_n \sim \frac{G}{s^2}\Bigg\{&(1+\exp(-2G))\left(\frac{\sqrt{\pi}\lambda}{2} - \frac{1}{G}\right) \\ &- (1-\exp(-2G))\left(\log(\lambda G) - \frac{\gamma}{2}\right) \\ &+ J_+ + \exp(-2G)J_-\Bigg\}, \qquad \lambda \gg 1\end{aligned} \tag{4.11}$$

where $\lambda = \sqrt{2}s/(G\sqrt{\beta}|n|T)$ (i.e., we allow large s and moderate values of nT), γ is the Euler's constant, and J_+ and J_- are the constants defined below (3.14).

Fig. 4 shows plots of the timing shift of the bits u_{-2}, u_{-1}, and u_1 for the bit pattern "1101" ($k = -2, -1, 0, 1$), obtained from (4.7) with (4.9) calculated numerically and from direct simulation of (2.1). In order to compute the timing shift of u_k, $k \neq 0$ using (4.7), we need to shift the bit pattern by $-kT$ so that the central position of u_k is moved to $t = 0$, and relabel all the bit slots correspondingly. Δt_{-2}, for instance, is given by $\Delta t_0(n = 1) + \Delta t_0(n = 3)$. Once again good agreement between the analytical and the numerical results can be seen. We also show the timing shift of u_{-2} in a lossless case obtained from direct simulation. As predicted, a significant suppression of the timing shift is observed even with the same value of path-average power as in the lossy case.

V. Timing and Amplitude Jitter

Explicit formulae to compute the timing shift at the chirp-free points (Δt_0) and the energy change (ΔW_0) were obtained by assuming that average dispersion is small and a signal u_k is periodic in z. When u_k is written as a Gaussian pulse (3.4), from

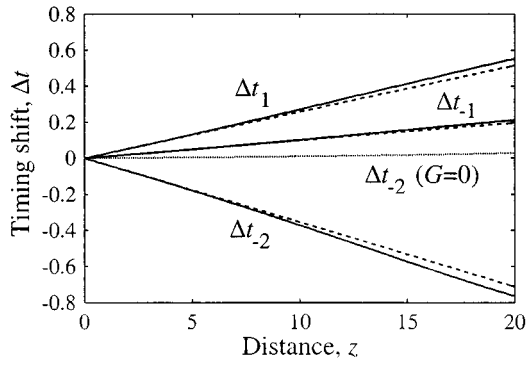

Fig. 4. Growth of timing shifts of the signals centered at $t = -2T$ (Δt_{-2}), $t = -T$ (Δt_{-1}) and $t = T$ (Δt_1) in a 1101 bit pattern in a lossy case ($\Gamma = 10$). The solid curves are the results of direct numerical simulation of (2.1) and the dashed curves are the results obtained from (4.7) with (4.10). The dotted curve shows the timing shift Δt_{-2} when $G = 0$ obtained from direct numerical simulation.

(4.7) with (4.9) and (3.7) with (3.10), the total amount of timing shift and energy change for a general bit pattern are given by

$$\Delta t_0(z) = \sum_{n=-N/2}^{N/2} b_n \overline{P}_n z \tag{5.1a}$$

$$\overline{P}_n = -\frac{\alpha^2 \beta n T}{\sqrt{2}\pi z_a} \int_0^{z_a} \frac{C(z) g(z)}{|\xi(z)|^3} \exp\left(-\frac{\beta n^2 T^2}{2|\xi(z)|^2}\right) dz \tag{5.1b}$$

$$\Delta W_0(z) = \sum_{n=-N/2}^{N/2} \sum_{m=-N/2}^{N/2} b_{m+n} b_m b_n \overline{Q}_{m,n} z \tag{5.2a}$$

$$\overline{Q}_{m,n} = -\frac{\alpha^4}{2\pi^2 z_a} \sqrt{\frac{\pi}{2\beta}} \int_0^{z_a} \mathrm{Im}\left[\frac{g(z)}{|\xi(z)|} \times \exp\left(-\frac{(m^2+n^2)\beta + 2imnC(z)}{2|\xi(z)|^2} T^2\right)\right] dz \tag{5.2b}$$

where b_k represents encoded binary data of the bit at $t = kT$ which takes either 1 or 0, and N is the total number of the interacting pulses. This is estimated as $N = (2/M)\sqrt{1 + (s/\beta)^2}$ where $M = t_{\mathrm{bit}}/\tau_{\mathrm{FWHM}} = 5$.

Because of a random sequence of bits b_k, Δt_0, and ΔW_0 are random variables and thus, (5.1) and (5.2) allow us to compute the mean value and the variance of Δt_0 and ΔW_0, which yields timing and amplitude jitter. Timing and amplitude jitter are given by the variance of the mean temporal position of pulses and the normalized energy variance, respectively

$$\sigma_t^2 = \langle t_0^2 \rangle - \langle t_0 \rangle^2 \tag{5.3}$$

$$\rho^2 \equiv \frac{\sigma_W^2}{W_0^2} = \frac{\langle W_0^2 \rangle - \langle W_0 \rangle^2}{W_0^2} \tag{5.4}$$

(here $\langle X \rangle$ denotes the mean value of the random variable X). Since b_k takes the value 1 and 0 with probability 1/2 from (5.1) and (5.2) we have

$$\sigma_t^2 = \langle (\Delta t_0)^2 \rangle - \langle \Delta t_0 \rangle^2 = \frac{z^2}{4} \sum_n \overline{P}_n^2 \tag{5.5}$$

$$\rho^2 = \frac{\langle (\Delta W_0)^2 \rangle - \langle \Delta W_0 \rangle^2}{W_0^2} = \frac{z^2}{W_0^2} \left[\frac{3}{16} \sum_n (\overline{Q}_{n,n}^2 + \overline{Q}_{n,n} \overline{Q}_{2n,2n}) + \frac{7}{64} \sum_{\substack{m,n \\ m \neq n}} \overline{Q}_{m,n}^2 + \sum_{\substack{n_1, m_2, n_2 \\ m_2 \neq n_2}} p_1 \overline{Q}_{n_1,n_1} \overline{Q}_{m_2,n_2} + \sum_{\substack{m_1, n_1, m_2, n_2 \\ m_1 \neq n_1, m_2 \neq n_2}} p_2 \overline{Q}_{m_1,n_1} \overline{Q}_{m_2,n_2} \right] \tag{5.6}$$

where all sums are taken from $-N/2$ to $N/2$, and $p_1 = 3/16$ or 1/16 if for each combination (n_1, m_2, n_2) there are three or four distinct elements, respectively, among the sequence $\{n_1, 2n_1, m_2, n_2, m_2 + n_2\}$, and $p_2 = 3/64$ or 1/64 if for each (m_1, n_1, m_2, n_2) there are four or five distinct elements, respectively, among $\{m_1, n_1, m_1 + n_1, m_2, n_2, m_2 + n_2\}$.

Calculation of σ_t and ρ allows one to estimate the bit error rate (BER) caused by timing and amplitude jitter without noise in the following way. Assuming that t_0 and W_0 follow Gaussian statistics, σ_t and ρ are individually related to BER through [18]

$$\mathrm{BER} = \mathrm{erfc}\left(\frac{\alpha t_{\mathrm{bit}}}{\sqrt{2\sigma_t^2}}\right) \tag{5.7}$$

$$\mathrm{BER} = \frac{1}{2}\,\mathrm{erfc}\left(\frac{Q}{\sqrt{2}}\right)$$

$$Q = \frac{I_{\mathrm{one}} - I_{\mathrm{zero}}}{\sigma_{\mathrm{one}} + \sigma_{\mathrm{zero}}} \approx \frac{I_{\mathrm{one}}}{\sigma_{\mathrm{one}}} = \frac{W_0}{\sigma_W} = \frac{1}{\rho} \tag{5.8}$$

where α (=0.2–0.4) measures the time-acceptance window size in the receiver, I_{one} (I_{zero}) and σ_{one} (σ_{zero}) are the mean value and standard deviation, respectively, in the level of one (zero) bit in the received eye diagram, and $\mathrm{erfc}(\cdot)$ is the complementary error function. In (5.8), we assumed $I_{\mathrm{zero}} = 0$ and $\sigma_{\mathrm{zero}} = 0$ by neglecting ghost pulse growth in the "0s." Based on this simple estimate, in order to achieve BER $< 10^{-9}$, σ_t and ρ must satisfy the condition $\sigma_t < 0.06 t_{\mathrm{bit}} = 1.5$ ps for $\alpha = 0.35$ and $\rho = 1/Q < 1/6 = 0.167$.

VI. Suppression by Distributed Amplification

It was found in Sections III and IV that in a DM system with GVD profile shown in Fig. 1, the growth rate of timing shift and energy change $\overline{P}_n = \overline{Q}_{m,n} = 0$ when $g(z) = 1$. This implies a substantial reduction of timing and amplitude jitter due to the intrachannel pulse interactions in a lossless system. This suppression is attributed to the absence of amplification, which introduces periodicity into the system and in turn brings

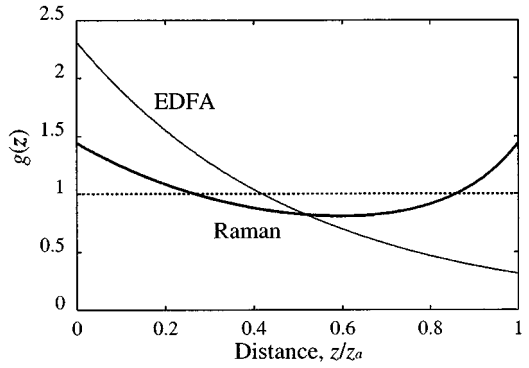

Fig. 5. Power variation of a pulse $g(z)$ within one dispersion management period with EDFA and Raman amplifiers. The dotted line is $\langle g \rangle$.

about strong resonance. It is impossible in practice to fabricate a lossless fiber; instead, employing distributed amplification is intuitively expected to be effective in reducing the intrachannel interactions since it can provide a nearly lossless transmission line by compensating loss more uniformly. Similar results are found when $\langle D \rangle$ is small but nonzero.

We compare two amplification models: lumped amplification based on EDFA (2.2) and distributed amplification based on backward Raman amplifiers. The nonlinear coefficient $g(z)$ for Raman amplifier is given by

$$g(z) = g_r \exp\{-2\Gamma(z - nz_a) + g_1[\exp(2\Gamma_p(z - nz_a)) - 1]\} \quad nz_a \le z < (n+1)z_a, \tag{6.1}$$

where $g_1 = 2\Gamma z_a \exp(-2\Gamma_p z_a)/[1 - \exp(-2\Gamma_p z_a)]$, Γ_p represents fiber loss at the pump wavelength, and g_r is determined so that $\langle g \rangle = 1$. The model (6.1) is obtained by solving coupled equations which describe the interaction between signal and pump power and neglecting the effect of pump depletion [21]. The two functions are plotted in Fig. 5. As can be seen, Raman amplification provides a more uniform distribution of power and effective nonlinearity than EDFA. We remark that the path-average peak power $\langle |u_k|^2_{\max} \rangle$ is assumed to be the same for EDFA and Raman amplification.

Fig. 6 shows plots of (a) timing jitter σ_t and (b) amplitude jitter ρ versus transmission distance in an EDFA and a Raman system when $z_a = 0.125$ and $s = 30$, corresponding to the period 50 km and $k'' = \pm 21.6\ \text{ps}^2/\text{km}$. The initial peak power is 2.72 mW for an EDFA system and 1.7 mW for a Raman system. Note that the comparison is made with the same value of path-average power (1 mW) in both systems. The fiber loss at the signal and pump wavelength is 0.22 dB/km and 0.28 dB/km, namely $\Gamma = 10$ and $\Gamma_p = 12.5$ respectively. Other parameters are the same as in Fig. 2. As predicted from the model in the previous section, both timing and amplitude jitter grow linearly with respect to distance in an EDFA system. A Raman system is especially effective in suppressing timing jitter. The insufficient suppression of amplitude jitter is due to the residual growth of ghost pulses [see (3.22)], which are generated from the signals, resulting in the leakage of their energy. The threshold required for error-free transmission based on the simple estimate [(5.7), (5.8) and below] is also plotted in this figure.

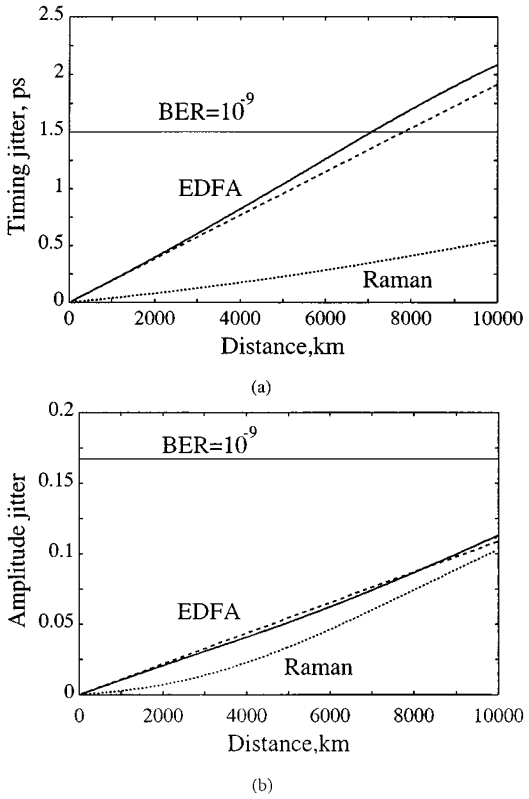

Fig. 6. Timing jitter σ_t (a) and amplitude jitter ρ (b) versus transmission distance for $s = 30$. The solid and dotted lines are the results of direct numerical simulation of (2.1) with $2^8 - 1$ PRBS bit pattern in an EDFA and Raman system, respectively, and the dashed lines are the analytical results for an EDFA system obtained from (5.5) and (5.6) with (5.1) and (5.2).

The analytical model obtained so far allows us to study how system performance is limited by intrachannel pulse interactions depending on the value of map strength. Fig. 7 shows the normalized growth rate of (a) timing and (b) amplitude jitter for various values of map strength obtained from (5.5) and (5.6) with (5.1) and (5.2) in a EDFA system. Timing jitter takes the largest value for moderate values of s ($\sim$15–20). For larger s, timing jitter decreases whereas amplitude jitter still remains to be a potential dominant cause of transmission penalty.

VII. Generalized Analytical Model: Multiple Scale Approach

In this section, using the multiple scale method, we unify the analytical framework which has been presented so far and show how to extend the previous results to more general situations where $\langle D \rangle \neq 0$ and/or the pulse is prechirped. The key idea behind multiple scale approach is to introduce fast and slow scales and thus, eliminate fast pulse dynamics due to large and periodically varying dispersion [19]. The leading order multiple scale approximation is found to agree with the analytical model presented in Sections III and IV.

We start the analysis with the perturbed NLS equation of the form

$$i\frac{\partial u_0}{\partial z} + \frac{D(z)}{2}\frac{\partial^2 u_0}{\partial t^2} = -g(z)|u_0|^2 u_0 - 2g(z)|u_j|^2 u_0 - g(z)u_l^* u_m u_n \tag{7.1}$$

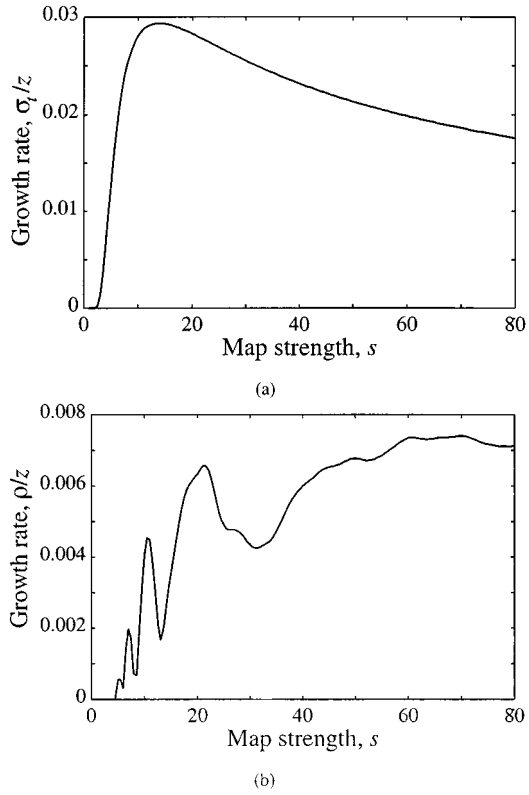

Fig. 7. Normalized growth rate of (a) timing jitter σ_t/z and (b) amplitude jitter ρ/z versus map strength s, obtained from (5.5) and (5.6) with (5.1) and (5.2) calculated numerically.

where the second and third term of the RHS is intrachannel XPM and FWM term, respectively, where $j \neq 0$ and $l = m+n$ ($m, n \neq 0$) from the phase-matching condition (3.3). In order to model strong dispersion management, we decompose the GVD $D(z)$ into two parts: a path-average constant $\langle D \rangle$ and a rapidly varying function Δ corresponding to local GVD

$$D(z) = \langle D \rangle + \frac{1}{z_a}\,\Delta(z/z_a) \tag{7.2}$$

where $z_a (\ll 1)$ is the map period. Note that Δ represents a large variation about the average due to strong dispersion management and thus, the proportionality factor $1/z_a$ is inserted in front of $\Delta(z/z_a)$. Both $\langle D \rangle$ and Δ are order one quantities. Since the perturbed NLS equation with $D(z)$ given by (7.2) contains both slowly and rapidly varying terms, it is convenient to introduce the fast and slow scales as $\zeta = z/z_a$ and z, respectively. We also expand the field u_k ($k = 0, l, m, n$) in powers of z_a

$$u_k(\zeta, z, t) = u_k^{(0)}(\zeta, z, t) + z_a u_k^{(1)}(\zeta, z, t) + \cdots. \tag{7.3}$$

The perturbed NLS equation is now broken into a series of equations corresponding to the different powers of z_a. At the leading order in the expansion $O(1/z_a)$, we have

$$i\,\frac{\partial u_k^{(0)}}{\partial \zeta} + \frac{\Delta(\zeta)}{2}\,\frac{\partial^2 u_k^{(0)}}{\partial t^2} = 0 \tag{7.4}$$

namely the evolution of the pulse is determined solely by the large variations of $D(z)$ about the average, and nonlinearity and residual dispersion represent only a small perturbation to the linear solution. Equation (7.4) can be solved by the Fourier transform and the solution is given by

$$\hat{u}_k^{(0)}(\zeta, z, \omega) = \hat{U}_k(z, \omega)\exp[-iC(\zeta)\omega^2/2] \tag{7.5}$$

where $C(\zeta) = \int_0^\zeta \Delta(\zeta')\,d\zeta'$, and $\hat{U}_k(z, \omega) = \hat{U}_0(z, \omega)\exp(i\omega kT)$ is the integration constant in terms of ζ and represents the slowly evolving amplitude of $\hat{u}_k^{(0)}$, whose exact form is determined from the higher order in the expansion.

At $O(1)$ in the expansion, for $u_0^{(1)}$ we have (in the frequency domain)

$$i\,\frac{\partial \hat{u}_0^{(1)}}{\partial \zeta} - \frac{\Delta(\zeta)}{2}\,\omega^2 \hat{u}_0^{(1)} = -\hat{F}^{(1)}(z, \omega) \tag{7.6a}$$

$$\begin{aligned}\hat{F}^{(1)}(z, \omega) &= i\,\frac{\partial \hat{u}_0^{(0)}}{\partial z} - \frac{\langle D \rangle}{2}\,\omega^2 \hat{u}_0^{(0)} \\ &\quad + g(z)\mathcal{F}\left[\left|u_0^{(0)}\right|^2 u_0^{(0)} + 2\left|u_j^{(0)}\right|^2 u_0^{(0)} + u_l^{(0)*} u_m^{(0)} u_n^{(0)}\right]\end{aligned} \tag{7.6b}$$

which is written in a more convenient form as

$$i\,\frac{\partial}{\partial \zeta}\left[\hat{u}_0^{(1)}\exp\left(iC\omega^2/2\right)\right] = -\hat{F}^{(1)}(z, \omega)\exp\left(iC\omega^2/2\right). \tag{7.7}$$

In order to remove secularities, namely to avoid resonant growth of $u_0^{(1)}$ so that the expansion of u in powers of z_a in (7.3) is remained to be well ordered, we require the following condition:

$$\int_0^1 \hat{F}^{(1)}(z, \omega)\exp\left(iC\omega^2/2\right)\,d\zeta = 0. \tag{7.8}$$

This condition yields the following equation for $\hat{U}$:

$$\begin{aligned} i\,\frac{\partial \hat{U}_0}{\partial z} - \frac{\langle D \rangle}{2}\,\omega^2 \hat{U}_0 &= -\left\langle g(\zeta)\exp\left(iC\omega^2/2\right)\left(\mathcal{F}\left[\left|u_0^{(0)}\right|^2 u_0^{(0)}\right]\right.\right. \\ &\quad \left.\left. + \mathcal{F}\left[2\left|u_j^{(0)}\right|^2 u_0^{(0)}\right] + \mathcal{F}\left[u_l^{(0)*} u_m^{(0)} u_n^{(0)}\right]\right)\right\rangle \\ &\equiv -\left(\hat{\mathcal{I}}_{\mathrm{SPM}} + \hat{\mathcal{I}}_{\mathrm{XPM}} + \hat{\mathcal{I}}_{\mathrm{FWM}}\right) \end{aligned} \tag{7.9}$$

where

$$\hat{\mathcal{I}}_{\mathrm{SPM}} = \int_{-\infty}^{\infty}\int_{-\infty}^{\infty} r(\omega_1\omega_2)\hat{U}_0(z, \omega+\omega_1)\hat{U}_0(z, \omega+\omega_2) \times \hat{U}_0^*(z, \omega+\omega_1+\omega_2)\,d\omega_1\,d\omega_2 \tag{7.10a}$$

$$\hat{\mathcal{I}}_{\mathrm{XPM}} = 2\int_{-\infty}^{\infty}\int_{-\infty}^{\infty} r(\omega_1\omega_2)\hat{U}_0(z, \omega+\omega_1)\hat{U}_j(z, \omega+\omega_2) \times \hat{U}_j^*(z, \omega+\omega_1+\omega_2)\,d\omega_1\,d\omega_2 \tag{7.10b}$$

$$\hat{\mathcal{I}}_{\mathrm{FWM}} = \int_{-\infty}^{\infty}\int_{-\infty}^{\infty} r(\omega_1\omega_2)\hat{U}_m(z, \omega+\omega_1)\hat{U}_n(z, \omega+\omega_2) \times \hat{U}_l^*(z, \omega+\omega_1+\omega_2)\,d\omega_1\,d\omega_2 \tag{7.10c}$$

and $r(\omega_1\omega_2) = [1/(2\pi)^2]\langle g(\zeta)\exp(iC(\zeta)\omega_1\omega_2)\rangle$ is a kernel representing the structure of the dispersion profile and a function

of s. In a lossless system (i.e., when $g(z)=1$), the kernel $r(x)$ for a two-step dispersion profile shown in Fig. 1 is found to be

$$r(x)=\frac{1}{(2\pi)^2}\,\frac{\sin sx}{sx}. \tag{7.11}$$

When $g(z)\neq 1$, the kernel $r(x)$ for the two-step dispersion map depends on the relative location of the amplifier within one dispersion map period ζ_a ($|\zeta_a|<1/2$) and θ [20]

$$\begin{aligned} r(x)=\frac{1}{2\pi^2}\,&\frac{G\exp(2G)}{(sx+2iG\theta)(sx-2iG(1-\theta))}\\ &\times[2sx\exp[2G(1+2\zeta_a)]\sin(sx-2iG(1-\theta))\\ &\quad+i\exp(2isx\zeta_a/\theta)\cosh(2G)(sx-2iG\theta(1-\theta))]. \end{aligned} \tag{7.12}$$

In particular, when $\theta=1/2$ and $\zeta_a=0$, (7.12) reduces to

$$\begin{aligned} r(x)=\frac{1}{(2\pi)^2}\,\frac{G}{(sx)^2+G^2}\,&[sx\sin(sx)\operatorname{csch}G+G\\ &+isx(1-\cos(sx)\operatorname{sech}G)]. \end{aligned} \tag{7.13}$$

If we keep only the term $\hat{\mathcal{I}}_{\rm SPM}$ in (7.9), this is reduced to the DMNLS equation obtained in [19], which governs the long-scale evolution of a single pulse in DM systems.

We now apply (7.9) to study nonlinear intrachannel interactions. Since the energy of u_0 is computed by $W_0=(1/2\pi)\int_{-\infty}^{\infty}|\hat{U}_0(z,\omega)|^2\,d\omega$ in the frequency domain, the energy change is obtained from

$$\begin{aligned} \frac{dW_0}{dz}&=\frac{1}{2\pi}\int_{-\infty}^{\infty}\left(\hat{U}_0^*\,\frac{\partial\hat{U}_0}{\partial z}+\hat{U}_0\,\frac{\partial\hat{U}_0^*}{\partial z}\right)d\omega\\ &=\frac{i}{2\pi}\int_{-\infty}^{\infty}\left(\hat{U}_0^*\hat{\mathcal{I}}_{\rm FWM}-\hat{U}_0\hat{\mathcal{I}}_{\rm FWM}^*\right)d\omega. \end{aligned} \tag{7.14}$$

When $\langle D\rangle=0$, this formula agrees with (3.7) (see Appendix B). Equation (7.14), however, provides a more general result when $\langle D\rangle\neq 0$ and the pulse is prechirped by the cumulative dispersion C_0. We compute W_0 by rewriting $\hat{U}(z,\omega)$ as

$$\tilde{U}(z,\omega)=\hat{U}(z,\omega)\exp\left[-i(C_0+\langle D\rangle z)\omega^2/2\right] \tag{7.15}$$

and substituting to $\mathcal{I}_{\rm FWM}$ (7.10c) and dW_0/dz (7.14). Furthermore, when we take a limit $s\to 0$, this equation allows one to describe the evolution of energy change in a highly dispersed system [13], [14], i.e., large and constant dispersion fibers.

Similarly, the frequency shift of u_0 is also computed from (7.9). Noting that the mean frequency is given by $\Omega_0=\int_{-\infty}^{\infty}\omega|\hat{U}_0|^2\,d\omega/\int_{-\infty}^{\infty}|\hat{U}_0|^2\,d\omega$, we find the frequency shift due to the XPM term to be calculated from

$$\begin{aligned} \frac{d\Omega_0}{dz}&=\frac{\int_{-\infty}^{\infty}\omega\left(\hat{U}_0^*\,\frac{\partial\hat{U}_0}{\partial z}+\hat{U}_0\,\frac{\partial\hat{U}_0^*}{\partial z}\right)d\omega}{\int_{-\infty}^{\infty}\left|\hat{U}_0\right|^2d\omega}\\ &=\frac{\int_{-\infty}^{\infty}i\omega\left(\hat{U}_0^*\hat{\mathcal{I}}_{\rm XPM}-\hat{U}_0\hat{\mathcal{I}}_{\rm XPM}^*\right)d\omega}{\int_{-\infty}^{\infty}\left|\hat{U}_0\right|^2d\omega}. \end{aligned} \tag{7.16}$$

When $\langle D\rangle=0$, this agrees with (4.2) with the RHS replaced by its path-average (see Appendix C). The timing shift of u_0 is then computed by substituting this to (4.5) and (4.6). The detailed analytical treatment of multiple scale approach will be presented in future publications.

VIII. Conclusion

We have developed an analytical model which clarifies fundamental properties of nonlinear intrachannel pulse interactions in quasi-linear DM transmission systems. Periodic dispersion management with small average dispersion results in a resonant situation because of periodic forcing due to lumped amplification [see (3.9)] supported by phase matching in the time domain (3.3). This energy exchange process is fundamentally analogous to nonlinear quartet resonance in dispersive waves (i.e., FWM) which appears in a variety field of physics and engineering such as those occur in water waves (cf. [22]). Simple analytical expressions to estimate timing and amplitude jitter are obtained and compared favorably with the result of direct numerical simulation of the full system. Substantial suppression of transmission penalties may be possible by the employment of distributed Raman amplification, which minimizes the resonant process. Finally, the multiple scale approach for nonlinear intrachannel interactions is expected to provide a unified analytical framework describing long-scale dynamics of intrachannel nonlinear effects.

Appendix A
Frequency Shifts Due to Intra-Channel FWM

In Section IV, we computed frequency and timing shifts due to phase-independent (intrachannel XPM) terms $|u_n|^2u_0$ ($n\neq 0$). We show here that frequency shift caused by phase-dependent (intrachannel FWM) terms $u_l^*u_mu_n$ ($l\neq m,\ n;\ m,\ n\neq 0$) vanishes and thus, they are not responsible for timing jitter. Differentiating $\Omega_0=\operatorname{Im}[\int_{-\infty}^{\infty}(\partial u_0/\partial t)u_0^*\,dt]/W_0$ with respect to z, from (2.4) we find

$$\frac{d\Omega_0}{dz}=-\frac{g(z)\int_{-\infty}^{\infty}\left(u_l^*u_mu_n\,\frac{\partial u_0^*}{\partial t}+\text{c.c.}\right)dt}{\int_{-\infty}^{\infty}|u_0|^2\,dt}. \tag{A.1}$$

For a signal given by a Gaussian pulse (3.4), (A.1) is written as

$$\begin{aligned} \frac{d\Omega_0}{dz}=&\frac{g(z)\alpha^2\beta(m+n)T}{2\sqrt{2}\pi|\xi(z)|^3}\exp\left[-\frac{\beta(m^2+n^2)T^2}{2|\xi(z)|^2}\right]\\ &\times\left\{\cos\left[\frac{mnC(z)T^2}{|\xi(z)|^2}\right]+\frac{C(z)}{\beta}\sin\left[\frac{mnC(z)T^2}{|\xi(z)|^2}\right]\right\}. \end{aligned} \tag{A.2}$$

Indeed when $m=0$, (A.2) is reduced to (4.8), i.e., $d\Omega_0/dz$ due to intrachannel XPM $|u_n|^2u_0$ ($n\neq 0$). Note that (A.2) now contains rapidly oscillating terms due to large mnT^2, which are negligible contributions to frequency shift once they are integrated with respect to z.

Appendix B
Energy Change Computed From DMNLS Equation

In Section VII, we derived the averaged equation (7.9) which describes the pulse dynamics and interactions over a slow scale. Here, we show that the energy change of u_0 due to interaction with u_l, u_m, u_n ($l=m+n;\ m,\ n\neq 0$) derived from (7.9) provides the same result as those obtained in Section III when $\langle D\rangle=0$.

Equation (7.14) yields

$$\begin{aligned}\frac{dW_0}{dz} =& \frac{i}{2\pi}\left\{\int_{-\infty}^{\infty} d\omega \hat{U}_0^*(z,\omega)\int_{-\infty}^{\infty} d\omega_1\, d\omega_2 r(\omega_1\omega_2)\right.\\ &\times \hat{U}_m(z,\omega+\omega_1)\hat{U}_n(z,\omega+\omega_2)\\ &\left.\times \hat{U}_l^*(z,\omega+\omega_1+\omega_2) - \text{c.c.}\right\}\\ =& \frac{i}{(2\pi)^3}\left\{\int_0^1 d\zeta g(\zeta)\int_{-\infty}^{\infty} d\omega_1\, d\omega_2\, d\omega \hat{U}_0^*(z,\omega)\right.\\ &\times \hat{U}_m(z,\omega+\omega_1)\hat{U}_n(z,\omega+\omega_2)\\ &\left.\times \hat{U}_l^*(z,\omega+\omega_1+\omega_2)\exp(iC\omega_1\omega_2) - \text{c.c.}\right\}\end{aligned} \tag{B.1}$$

where we referred to the definition of the kernel $r(\omega_1\omega_2) = [1/(2\pi)^2]\int_0^1 d\zeta g(\zeta)\exp(iC(\zeta)\omega_1\omega_2)$. From (7.5), we have $\hat{U}_k(z,\omega) = \hat{u}_k^{(0)}(\zeta, z, \omega)\exp[iC(\zeta)\omega^2/2]$ and obtain

$$\begin{aligned}\frac{dW_0}{dz} =& \frac{i}{(2\pi)^3}\int_0^1 d\zeta g(\zeta)\int_{-\infty}^{\infty} d\omega_1\, d\omega_2\, d\omega\\ &\left[\hat{u}_0^*(\zeta,z,\omega)\exp(-iC\omega^2/2)\hat{u}_m(\zeta,z,\omega+\omega_1)\right.\\ &\times \exp(iC(\omega+\omega_1)^2/2)\hat{u}_n(\zeta,z,\omega+\omega_2)\\ &\times \exp(iC(\omega+\omega_2)^2/2)\hat{u}_l^*(\zeta,z,\omega+\omega_1+\omega_2)\\ &\left.\times \exp(-iC(\omega+\omega_1+\omega_2)^2/2)\exp(iC\omega_1\omega_2) - \text{c.c.}\right]\\ =& \frac{i}{(2\pi)^3}\int_0^1 d\zeta g(\zeta)\int_{-\infty}^{\infty} d\omega_1\, d\omega_2\, d\omega\\ &\times [\hat{u}_0^*(\zeta,z,\omega)\hat{u}_m(\zeta,z,\omega+\omega_1)\hat{u}_n(\zeta,z,\omega+\omega_2)\\ &\times \hat{u}_l^*(\zeta,z,\omega+\omega_1+\omega_2) - \text{c.c.}].\end{aligned} \tag{B.2}$$

By employing the inverse Fourier transform, we find

$$\begin{aligned}\frac{dW_0}{dz} =& \frac{i}{(2\pi)^3}\int_0^1 d\zeta g(\zeta)\int_{-\infty}^{\infty} dt_1\, dt_2\, dt_3\, dt_4\, d\omega_1\, d\omega_2\, d\omega\\ &\times \{u_0^*(\zeta,z,t_1)u_m(\zeta,z,t_2)u_n(\zeta,z,t_3)u_l^*(\zeta,z,t_4)\\ &\times \exp[-i\omega(-t_1+t_2+t_3-t_4)]\exp[-i\omega_1(t_2-t_4)]\\ &\times \exp[-i\omega_2(t_3-t_4)] - \text{c.c.}\}\\ =& i\int_0^1 d\zeta g(\zeta)\int_{-\infty}^{\infty} dt[u_0^*(\zeta,z,t)u_m(\zeta,z,t)\\ &\times u_n(\zeta,z,t)u_l^*(\zeta,z,t) - \text{c.c.}]\end{aligned} \tag{B.3}$$

where we used the identity $\int_{-\infty}^{\infty} d\omega \exp(i\omega t) = 2\pi\delta(t)$, and $t = t_1$. Energy change $\Delta W_0(z) = W_0(z) - W_0(0)$ is computed by integration of (B.3). When $\langle D\rangle = 0$, $\hat{u}_k$ is independent of z, so that the RHS of (B.3) is constant in terms of z, and thus ΔW_0 grows linearly with respect to distance

$$\begin{aligned}\Delta W_0(z) =& \overline{Q}_{m,n} z\\ \overline{Q}_{m,n} =& i\int_0^1 d\zeta g(\zeta)\int_{-\infty}^{\infty} dt\\ &\times [u_0^*(\zeta,t)u_m(\zeta,t)u_n(\zeta,t)u_l^*(\zeta,t) - \text{c.c.}]\end{aligned} \tag{B.4}$$

representing the growth rate. The obtained formula agrees with (3.6) and (3.7).

Appendix C
Frequency Shift Computed From DMNLS Equation

The averaged equation (7.9) derived in Section VII also provides an analytical framework which allows one to compute the frequency shift of u_0 due to interaction with u_j ($j \neq 0$). Here, we compute the frequency shift from (7.9) and show that when $\langle D\rangle = 0$ this gives the same result as those obtained in Section IV.

The numerator of (7.16) yields

$$\begin{aligned}&\int_{-\infty}^{\infty} i\omega\left(\hat{U}_0^*\hat{\mathcal{I}}_{\text{XPM}} - \hat{U}_0\hat{\mathcal{I}}_{\text{XPM}}^*\right)d\omega\\ &= 2\left\{\int_{-\infty}^{\infty} d\omega i\omega \hat{U}_0^*(z,\omega)\int_{-\infty}^{\infty} d\omega_1\, d\omega_2 r(\omega_1\omega_2)\right.\\ &\quad\times \hat{U}_0(z,\omega+\omega_1)\hat{U}_j(z,\omega+\omega_2)\\ &\quad\left.\times \hat{U}_j^*(z,\omega+\omega_1+\omega_2) - \text{c.c.}\right\}\\ &= \frac{2}{(2\pi)^2}\left\{\int_0^1 d\zeta g(\zeta)\int_{-\infty}^{\infty} d\omega_1\, d\omega_2\, d\omega i\omega\right.\\ &\quad\times \hat{U}_0^*(z,\omega)\hat{U}_0(z,\omega+\omega_1)\hat{U}_j(z,\omega+\omega_2)\\ &\quad\left.\times \hat{U}_j^*(z,\omega+\omega_1+\omega_2)\exp(iC\omega_1\omega_2) - \text{c.c.}\right\}\end{aligned} \tag{C.1}$$

where we referred to the definition of the kernel $r(\omega_1\omega_2) = [1/(2\pi)^2]\int_0^1 d\zeta g(\zeta)\exp(iC(\zeta)\omega_1\omega_2)$. From (7.5), we have

$$\begin{aligned}&\int_{-\infty}^{\infty} i\omega\left(\hat{U}_0^*\hat{\mathcal{I}}_{\text{XPM}} - \hat{U}_0\hat{\mathcal{I}}_{\text{XPM}}^*\right)d\omega\\ &= \frac{2}{(2\pi)^2}\int_0^1 d\zeta g(\zeta)\int_{-\infty}^{\infty} d\omega_1\, d\omega_2\, d\omega i\omega\\ &\quad\times [\hat{u}_0^*(\zeta,z,\omega)\exp(-iC\omega^2/2)\hat{u}_0(\zeta,z,\omega+\omega_1)\\ &\quad\times \exp(iC(\omega+\omega_1)^2/2)\hat{u}_j(\zeta,z,\omega+\omega_2)\\ &\quad\times \exp(iC(\omega+\omega_2)^2/2)\hat{u}_j^*(\zeta,z,\omega+\omega_1+\omega_2)\\ &\quad\times \exp(-iC(\omega+\omega_1+\omega_2)^2/2)\exp(iC\omega_1\omega_2) - \text{c.c.}]\\ &= \frac{2}{(2\pi)^2}\int_0^1 d\zeta g(\zeta)\int_{-\infty}^{\infty} d\omega_1\, d\omega_2\, d\omega i\omega\\ &\quad\times [\hat{u}_0^*(\zeta,z,\omega)\hat{u}_0(\zeta,z,\omega+\omega_1)\hat{u}_j(\zeta,z,\omega+\omega_2)\\ &\quad\times \hat{u}_j^*(\zeta,z,\omega+\omega_1+\omega_2) - \text{c.c.}].\end{aligned} \tag{C.2}$$

By employing the inverse Fourier transform, we find

$$\begin{aligned}&\int_{-\infty}^{\infty} i\omega\left(\hat{U}_0^*\hat{\mathcal{I}}_{\text{XPM}} - \hat{U}_0\hat{\mathcal{I}}_{\text{XPM}}^*\right)d\omega\\ &= \frac{2}{(2\pi)^2}\int_0^1 d\zeta g(\zeta)\int_{-\infty}^{\infty} dt_1\, dt_2\, dt_3\, dt_4\, d\omega_1\, d\omega_2\, d\omega i\omega\\ &\quad\times \{u_0^*(\zeta,z,t_1)u_0(\zeta,z,t_2)u_j(\zeta,z,t_3)u_j^*(\zeta,z,t_4)\\ &\quad\times \exp[-i\omega(-t_1+t_2+t_3-t_4)]\exp[-i\omega_1(t_2-t_4)]\\ &\quad\times \exp[-i\omega_2(t_3-t_4)] - \text{c.c.}\}\\ &= 2\int_0^1 d\zeta g(\zeta)\int_{-\infty}^{\infty} dt_1\, dt_4\end{aligned}$$

$$\times \left[u_0^*(t_1) u_0(t_4) |u_j(t_4)|^2 \int_{-\infty}^{\infty} d\omega i\omega \exp[i\omega(t_1 - t_4)] - u_0(t_1) u_0^*(t_4) |u_j(t_4)|^2 \int_{-\infty}^{\infty} d\omega i\omega \times \exp[-i\omega(t_1 - t_4)] \right]$$

$$= -2(2\pi) \int_0^1 d\zeta g(\zeta) \int_{-\infty}^{\infty} dt_4 \times \left(\frac{\partial u_0^*}{\partial t_4} u_0(t_4) + \frac{\partial u_0}{\partial t_4} u_0^*(t_4) \right) |u_j(t_4)|^2$$

$$= -2(2\pi) \int_0^1 d\zeta g(\zeta) \int_{-\infty}^{\infty} dt \frac{\partial |u_0|^2}{\partial t} |u_j|^2$$

$$= 2(2\pi) \int_0^1 d\zeta g(\zeta) \int_{-\infty}^{\infty} dt |u_0|^2 \frac{\partial |u_j|^2}{\partial t} \tag{C.3}$$

where we have used the relations $\int_{-\infty}^{\infty} d\omega \exp(i\omega t) = 2\pi\delta(t)$

$$\int_{-\infty}^{\infty} dt' f(t') \int_{-\infty}^{\infty} d\omega i\omega \exp[\pm i\omega(t' - t)] = \mp 2\pi \int_{-\infty}^{\infty} dt' (df/dt') \delta(t' - t) = \mp 2\pi (df/dt),$$

and $t = t_4$. Thus $d\Omega_0/dz$ is obtained from (7.16) and (C.3) as

$$\frac{d\Omega_0}{dz} = 2 \int_0^1 d\zeta g(\zeta) \frac{\int_{-\infty}^{\infty} |u_0(\zeta, z, t)|^2 \frac{\partial}{\partial t} |u_j(\zeta, z, t)|^2 \, dt}{\int_{-\infty}^{\infty} |u_0(\zeta, z, t)|^2 \, dt} \tag{C.4}$$

where we used

$$\int_{-\infty}^{\infty} \left| \hat{U}_0(z, \omega) \right|^2 d\omega = \int_{-\infty}^{\infty} |\hat{u}_0(\zeta, z, \omega)|^2 \, d\omega = 2\pi \int_{-\infty}^{\infty} |u_0(\zeta, z, t)|^2 \, dt.$$

Note that when $\langle D \rangle = 0$, $\hat{u}_k$ is independent of z, so that the RHS of (C.4) is constant in terms of z. Thus the frequency shift $\Delta\Omega_0 = \Omega_0(z) - \Omega_0(0)$ grows linearly with respect to distance, and the growth rate is given by

$$\overline{S}_n = 2 \int_0^1 d\zeta g(\zeta) \frac{\int_{-\infty}^{\infty} |u_0(\zeta, t)|^2 \frac{\partial}{\partial t} |u_j(\zeta, t)|^2 \, dt}{\int_{-\infty}^{\infty} |u_0(\zeta, t)|^2 \, dt} \tag{C.5}$$

which is the path average of the RHS of (4.2).

ACKNOWLEDGMENT

The authors would like to acknowledge A. Docherty for providing useful remarks.

REFERENCES

[1] M. J. Ablowitz, T. Hirooka, and G. Biondini, "Quasilinear optical pulses in strongly dispersion managed transmission systems," *Opt. Lett.*, vol. 26, pp. 459–461, 2001.

[2] M. J. Ablowitz and T. Hirooka, "Managing nonlinearity in strongly dispersion-managed optical pulse transmission," *J. Opt. Soc. Amer. B*, vol. 11, pp. 425–439, 2002.

[3] C. Kurtzke, "Suppression of fiber nonlinearities by appropriate dispersion management," *IEEE Photon. Technol. Lett.*, vol. 5, pp. 1250–1253, Oct. 1993.

[4] R. W. Tkach, A. R. Chraplyvy, F. Forghieri, A. H. Gnauck, and R. M. Derosier, "Four photon mixing and high-speed WDM systems," *IEEE J. Lightwave Technol.*, vol. 13, pp. 841–849, May 1995.

[5] N. S. Bergano, C. R. Davidson, M. Ma, A. Pillipetskii, S. G. Evangelides, H. D. Kidorf, J. M. Darcie, E. Golovchenko, K. Rottwitt, P. C. Corbett, R. Menges, M. A. Mills, B. Pedersen, D. Peckham, A. A. Abramov, and A. M. Vengsarkar, "Digest of optical fiber communication conference," in *Opt. Soc. Amer.*, Washington, DC, 1998, Postdeadline Paper PD12.

[6] R. J. Essiambre, B. Mikkelsen, and G. Raybon, "Intra-channel cross-phase modulation and four-wave mixing in high-speed TDM systems," *Electron. Lett.*, vol. 35, pp. 1576–1578, 1999.

[7] P. V. Mamyshev and N. A. Mamysheva, "Pulse-overlapped dispersion managed data transmission and intrachannel four wave mixing," *Opt. Lett.*, vol. 24, pp. 1454–1456, 1999.

[8] J. Martensson, A. Berntson, M. Westlund, A. Danielsson, P. Johannisson, D. Anderson, and M. Lisak, "Timing jitter owing to intrachannel pulse interactions in dispersion managed transmission systems," *Opt. Lett.*, vol. 26, pp. 55–57, 2001.

[9] S. Kumar, "Intrachannel four wave mixing in dispersion managed RZ systems," *IEEE Photon. Technol. Lett.*, vol. 13, pp. 800–802, Aug. 2001.

[10] M. J. Ablowitz and T. Hirooka, "Intra-channel pulse interactions in dispersion managed systems: Timing shifts," *Opt. Lett.*, vol. 26, pp. 1846–1848, 2001.

[11] ——, "Intra-channel pulse interactions in dispersion managed systems: energy transfer," *Opt. Lett.*, vol. 27, pp. 203–205, 2002.

[12] ——, "Resonant nonlinear intrachannel interactions in strongly dispersion managed transmission systems," *Opt. Lett.*, vol. 25, pp. 1750–1752, 2000.

[13] A. Mecozzi, C. B. Claussen, and M. Shtaif, "Analysis of intrachannel nonlinear effects in highly dispersed optical pulse transmission," *IEEE Photon. Technol. Lett.*, vol. 12, pp. 392–394, Apr. 2000.

[14] ——, "System impact on intra-channel nonlinear effects in highly dispersed optical pulse transmission," *IEEE Photon. Technol. Lett.*, vol. 12, pp. 1633–1635, Dec. 2000.

[15] R.-M. Mu and C. R. Menyuk, "Symmetric slope compensation in a long haul WDM system using the CRZ format," *IEEE Photon. Technol. Lett.*, vol. 13, pp. 797–799, Aug. 2001.

[16] M. J. Ablowitz, G. Biondini, S. Chakravarty, R. B. Jenkins, and J. R. Sauer, "Four wave mixing in wavelength-division-multiplexed soliton systems: Damping and amplification," *Opt. Lett.*, vol. 21, pp. 1646–1648, 1996.

[17] A. Mecozzi, C. B. Clausen, M. Shtaif, S. G. Park, and A. H. Gnauck, "Cancellation of timing and amplitude jitter in symmetric links using highly dispersed pulses," *IEEE Photon. Technol. Lett.*, vol. 13, pp. 445–447, May 2001.

[18] E. Iannone, F. Matera, A. Mecozzi, and M. Settembre, *Nonlinear Optical Communication Networks*. New York: Wiley, 1998.

[19] M. J. Ablowitz and G. Biondini, "Multiscale pulse dynamics in communication systems with strong dispersion management," *Opt. Lett.*, vol. 23, pp. 1668–1670, 1998.

[20] M. J. Ablowitz, G. Biondini, and E. S. Olson, "On the evolution and interaction of dispersion managed solitons," in *Massive WDM and TDM Soliton Transmission Systems*, Ed. A. Hasegawa, Ed. Dordrecht, The Netherlands: Kluwer, 2000.

[21] G. P. Agrawal, *Nonlinear Fiber Optics*, 3rd ed. New York: Academic, 2001.

[22] A. C. Newell, S. Nazarenko, and L. Biven, "Water turbulence and intermittency," *Physica D*, vol. 152–153, pp. 520–550, 2001.

Mark J. Ablowitz received the Ph.D. degree in mathematics from Massachusetts Institute of Technoogy, Cambridge, MA, in 1971.

He is currently a professor of applied mathematics at the University of Colorado at Boulder, CO. He was an Alfred P. Sloan Foundation Research Fellow in 1976 and a John Simon Guggenheim Foundation Fellow in 1984.

Dr. Ablowitz is a member of the American Mathematical Society (AMS), Society for Industrial and Applied Mathematics (SIAM), and Optical Society of America (OSA).

Toshihiko Hirooka (M'00) was born in Osaka, Japan on December 9, 1974. He received the Ph.D. degree in electronic and information systems engineering from Osaka University, Osaka, Japan, in 2000.

He is currently a research associate at Department of Applied Mathematics, University of Colorado at Boulder, CO. His research interests include nonlinear optics and fiber-optic communications.

Dr. Hirooka is a member of Optical Society of America (OSA), and the Institute of Electronics, Information, and Communication Engineers (IEICE) of Japan.